Light-Induced Electron Spin Polarization in Vanadyl Octaethylporphyrin: II. Dynamics of the Excited States

Yuri E. Kandrashkin,[†,‡] Motoko S. Asano,[§,||] and Art van der Est*[,†]

Department of Chemistry, Brock University, 500 Glenridge Ave. St. Catharines Onterio, Canada L2S 3A1, Kazan Physical-Technical Institute Russian Academy of Sciences, Kazan, Russian Federation, and Department of Chemistry, Tokyo Institute of Technology, O-okayama, Meguro-ku, Tokyo 152-8551, Japan

Received: April 2, 2006; In Final Form: June 6, 2006

The dynamics of the low-lying excited states of vanadyl octaethylporphyrin (OEPVO) in frozen solution is investigated by transient electron paramagnetic resonance (TREPR). The observation of spin-polarized TREPR spectra from the lowest excited trip-quartet state of OEPVO, reported in the preceding paper, opens a new avenue for investigation of the excited states of such molecules. Here, a model based on the back-and-forth transitions between the trip-quartet and trip-doublet states is developed and used to explain the time dependence of the low-temperature laser flash-induced electron spin polarization of OEPVO. At early times, the TREPR spectra show predominantly multiplet polarization, whereas strong net polarization develops at later times. An analysis of the time dependence reveals two well-separated processes: (i) fast evolution of the polarization from the multiplet pattern to the net absorptive pattern and (ii) very slow decay of the net polarization. Both processes are temperature dependent and are faster at higher temperature. All of these observed features can be reproduced, and the experimental data can be simulated within the framework of the model. For simplicity, only the two nearly degenerate orbital states resulting from the $a_1 \rightarrow e$ triplet excitation of the porphyrin are considered. Each of these is split into a trip-doublet and trip-quartet giving a total of four low-lying excited states. Transitions between the trip-doublet and trip-quartet states are assumed to be governed by spin−orbit coupling, which mixes the four low-lying states. It is known that following light excitation, the molecule initially decays to the lowest trip-doublet state and then to the trip-quartet state. In agreement with the observed TREPR spectra, the model predicts that this decay results in predominantly multiplet polarization of the trip-quartet. However, a small amount of net polarization is also predicted due to the spin selectivity associated with the Zeeman interaction. Because the energy gap between the trip-doublet and trip-quartet states is small, back-and-forth electronic transitions between the trip-doublet and trip-quartet are expected to occur as thermal equilibrium is established. The model predicts that it is these transitions that lead to the observed evolution of the initial multiplet polarization to net absorptive polarization.

1. Introduction

An important feature of most light-induced processes is the role that the electron spin can play in the excited-state dynamics. Despite the fact that the energy associated with the spin angular momentum is usually many orders of magnitude smaller than the electrostatic energies, processes such as electronic relaxation, energy transfer, and electron transfer are often spin-selective. This spin selectivity arises because of the exchange interaction, which has a significant effect on the energies of the excited states, and because of the spin−orbit coupling, which influences the transitions between them. As a result, the paramagnetic excited states generated by light excitation usually exhibit electron spin polarization, which can be detected using transient electron paramagnetic resonance spectroscopy (TREPR).[1−7] Although the excited-state dynamics are often too fast to be observed directly by EPR methods, the polarization patterns depend on the energetics and relaxation pathways and can be used to study these properties indirectly.[4,8−22] In paramagnetic metal complexes, the polarization is usually detected in the ground state[10,19,23] or in the excited state of a chromophore that is relatively weakly coupled to the metal.[9,21,22]

Recently, however, we made the first report[24] of spin polarization in the excited quartet state of vanadyl octaetylporphyrin (OEPVO). The vanadyl ion has a d^1 electronic configuration, and hence, vanadyl porphyrin has a doublet ground state and doublet and quartet $\pi-\pi^*$ excited states. Using the terminology introduced by Gouterman,[25] we will refer to these electronic states as "sing-doublet", "trip-doublet", and "trip-quartet", where "sing" and "trip" indicate singlet and triplet multiplicities of the $\pi-\pi^*$ excitation whereas doublet and quartet indicate the total spin multiplicity. In the preceding paper,[26] we presented an analysis of the orientation dependence and lifetime of the spin polarization patterns of OEPVO observed below 80 K and obtained the magnetic resonance

* To whom correspondence should be addressed. E-mail: avde@brocku.ca. FAX: 905-682-9020.
[†] Brock University.
[‡] Kazan Physical-Technical Institute Russian Academy of Sciences.
[§] Tokyo Institute of Technology.
[||] Current address: Department of Chemistry, Graduate School of Science and Engineering, Tokyo Metropolitan University 1−1, Minami-Ohsawa, Hachi-Ohji, Tokyo 192-0397, Japan.

10.1021/jp062037x CCC: $33.50
Published on Web 07/19/2006

parameters of the trip-quartet state and the energy gap between the trip-quartet and trip-doublet states.

An unusual feature of the spin polarization patterns is the strong net polarization and relatively weak multiplet contribution. This observation is hard to rationalize within the framework of standard models for the generation of spin polarization[27] because intramolecular transitions, which are governed by the molecular symmetry, produce strong multiplet polarization. Other mechanisms involving diffusion and level-crossing can be excluded because of the low temperature of the experiment and strong spin−spin coupling in the molecule. Recently, we developed a model to describe the polarization associated with doublet-quartet intersystem crossing in such systems.[14] The model assumes that relaxation occurs rapidly to the lowest trip-doublet from which intersystem crossing to the lowest trip-quartet takes place. The intersystem crossing rate depends on the degree of doublet−quartet mixing induced by spin−orbit coupling. Because the spin state energies depend on orientation of the magnetic field, spin−orbit coupling acts differently on states with parallel and antiparallel spin projections. Thus, the rates of ISC for the spin states are different due to breaking of the molecular symmetry by the external magnetic field. The difference in the rates then results in net polarization of the quartet state. However, this polarization is much weaker than the multiplet polarization associated with the spin−spin interaction.

In this paper, we investigate a possible mechanism by which the strong net polarization observed for OEPVO could develop. From measurements at 15 K in two solvents, we are able to clearly distinguish two patterns and extract their dynamics. The spectra show complex temporal behavior of these contributions. The first pattern, which shows multiplet polarization, develops within the rise time of the spectrometer and then decays and changes sign in the range of tens of microseconds. The second pattern shows net polarization several times more intense than the multiplet polarization. This contribution rises within the first several microseconds and decays with the lifetime of the trip-quartet.

The observed behavior can be understood within a model in which the net polarization develops during thermal equilibration between the trip-doublet and trip-quartet state. Such an equilibration between these states was first proposed by Gouterman[25] and later by Asano et al.[28] to explain the temperature dependence of the luminescence lifetime. We suggest that during the equilibration, the Zeeman interaction acts as a source of net polarization as invoked previously to explain the observations for relatively weakly coupled triplet−doublet pairs.[29,30] More recently, we showed from a perturbation theory treatment that it can also lead to observable changes in the spin polarization patterns in strongly coupled systems[13,14] and is probably responsible for the light-induced net polarization of the ground state of copper porphyrins.[10] We postulate that the combination of this effect and the back-and-forth transitions between the trip-quartet and trip-doublet leads to accumulation of net polarization. Here, we examine this idea more closely and present a detailed description of the associated kinetics.

2. Experimental Section

Details of the sample preparation and experimental conditions used to measure the spin polarization patterns and EPR spectra of the ground state along with the procedure used to simulate the spectra are described in the preceding paper.[26] In addition to the simulation of the spectra, the time dependence of the experimental polarization was obtained by fitting the spectrum at each time point and plotting the amplitudes of the components. The corresponding calculation of the time dependence on the basis of a kinetic model is described in the text below.

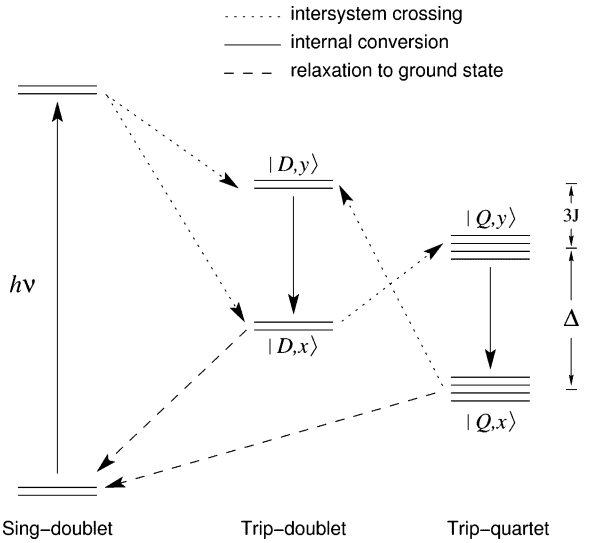

Figure 1. A simplified Jablonski diagram of OEPVO showing the low-lying states of the sing-doublet, trip-doublet, and trip-quartet manifolds. The relative energies of the states is not to scale, and the energy differences between the trip-doublet and trip-quartet states has been greatly expanded. The labels *x* and *y* refer to states derived from excitation of an electron from the HOMO into the e_x and e_y orbitals, respectively.

3. Results and Analysis

Before discussing the model for the evolution of the spin polarization in OEPVO, we first summarize the characteristics of the observed TREPR data and briefly review the evidence for the assignment of the spin polarization to the trip-quartet state. The description of the polarization patterns in terms of net and multiplet contributions presented in the preceding paper[26] is then extended to extract the time and temperature dependence of these contributions. The results of this analysis will be used in the subsequent section to specify the properties of the model.

3.1. Observable States. A simplified Jablonski diagram of OEPVO is presented in Figure 1, which shows all of the states that, in principle, could contribute to the observed spin polarization. The absorption of a photon near $\lambda = 500$ nm causes a $\pi-\pi^*$ singlet excitation of the porphyrin ring and initially populates the lowest excited sing-doublet state. Rapid ISC from this state then populates the corresponding trip-doublet and trip-quartet states. The lowest triplet $\pi-\pi^*$ excitation of octaelthylporphyrins has symmetry a_1e and is doubly degenerate. Hence, there are two low-lying trip-doublet and two trip-quartet states for OEPVO. We label these as D_x, D_y, Q_x, and Q_y (see Figure 1) to indicate the direction of the transition dipole. (Note that the relationship between the directions of the transition dipoles and the in-plane axes of the magnetic interactions has not been established and the labels should not be taken to imply that they coincide.) Because it is likely that the degeneracy is partially lifted, these states are shown in Figure 1 as having different energies. The low-temperature luminescence lifetimes of vanadyl porphyrins in the range of hundreds of microseconds suggest that the spin polarization arises from some combination of these four states. However, the ground sing-doublet state is also EPR active and could become polarized by the excitation and decay.[10,19] Hence, it must also be considered.

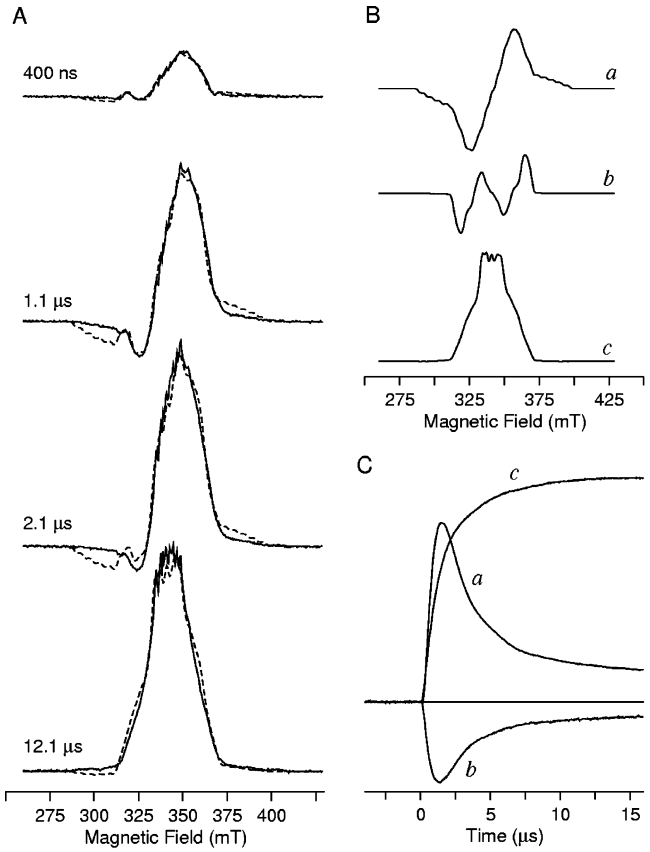

Figure 2. X-band (9 GHz) spin-polarized transient EPR spectra of vanadyl octaethylporphyin measured in toluene at 15 K after the light excitation. The spectra were measured using direct detection, and positive signals represent microwave absorption whereas negative signals are emission. (A) TREPR spectra in a series of 200-ns wide time windows centered at the times indicated beside the spectra. The time windows were chosen to demonstrate the evolution of the polarization after the light excitation. The amplitdues of the spectra have not been scaled relative to one another and show that the net polarization is the dominant contribution. The solid curves are the experimental spectra and the dashed curves are simulations of the tip-quartet state using spin-Hamiltonian (eq 1) and density matrix (eq 4) (for details, refer to text). The magnetic resonance parameters, used for simulations, and normalized weights of different contributions are listed in Tables 1−3. (B) Three contributions to the polarization patterns corresponding to the terms of density matrix (eq 4). (a) axial multiplet contribution, (b) nonaxial multiplet contribution, and (c) net contribution. (C) Time dependence of the contributions shown in (B) obtained by fitting the complete time/field dataset.

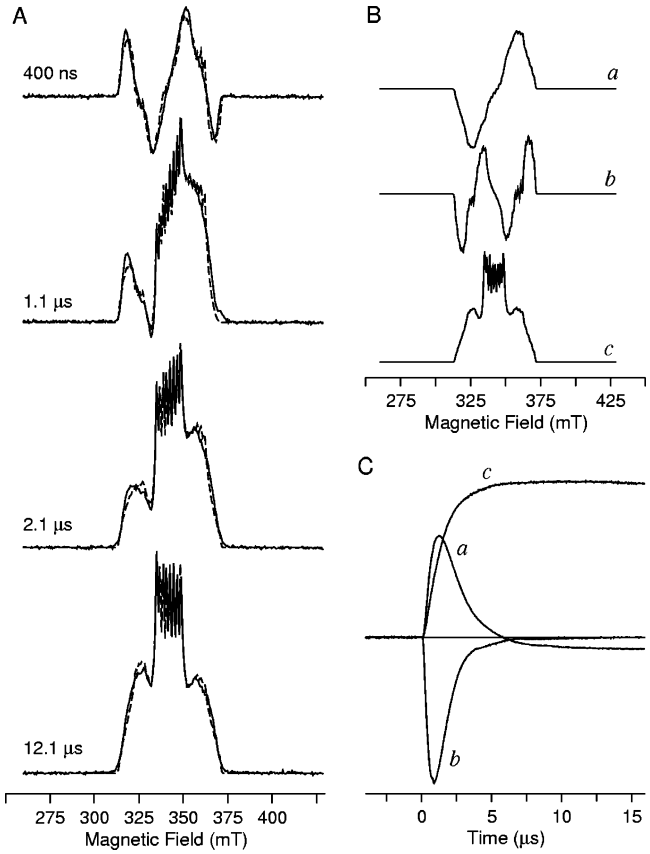

Figure 3. X-band (9 GHz) spin-polarized transient EPR spectra of vanadyl octaethylporphyin in the liquid crystal E7 with the director oriented parallel to the magnetic field. The spectra are taken under the same conditions and calculated as those shown in Figure 2, except that the orientational ordering with $S_{zz} = -0.4$ has been taken into account.

Figures 2−4 show light-induced electron spin polarization of OEPVO at 15 K. In Figure 2, the solvent is toluene, whereas in Figures 3 and 4, it is the liquid crystal E7 with the director oriented parallel and perpendicular to the external magnetic field, respectively. In each of the figures, panel A (left) shows experimental TREPR spectra (solid curves) in a series of 200-ns time windows chosen to illustrate the evolution of the predominantly multiplet polarization at early time to stronger net polarization at later times.

The assignment of the observed polarization patterns was addressed in detail in the preceding paper,[26] and they were identified as arising from the lowest trip-quartet state. Here, we summarize briefly the features that support this conclusion. First, at early times a multiplet pattern is observed. At low temperature in a rigid system with strongly coupled spin, such a pattern requires an overall spin multiplicity larger than $^1/_2$, and of the possible states, only the trip-quartet fulfils this requirement. Second, all components of the hyperfine splittings of both the multiplet pattern and the net polarization seen at later times are a factor of 3 smaller than those found from steady-state measurements of the ground state. This reduction is consistent with the expected reduction of the average spin density at the vanadium nucleus in an excited state with three unpaired electrons. Finally, both patterns can be simulated with the same set of parameters for the quartet state. Inclusion of a contribution from the trip-doublet or ground sing-doublet does not improve the quality of the simulation. Therefore, it is clear that both the net and multiplet polarization patterns arise predominantly from the lowest trip-quartet.

The main issue we wish to address here is how the spin polarization is generated initially and how the net polarization seen at late times develops. For this purpose, it is useful to divide the observed polarization into contributions with specific symmetry properties that can then be associated with the different possible interactions. These contributions also act as a good test of any model because they must correctly predict their time dependence.

3.2. Contributions to the Spin Polarization. The EPR signals of the trip-quartet state can be described using a spin Hamiltonian that includes the Zeeman interaction ω with external magnetic field B, the zero-field splitting given by the parameters D and E, and the hyperfine interaction described by the tensor **A**:

$$H = \omega S_z + D(S_{\Omega,z}^2 - \vec{S}^2) + E(S_{\Omega,x}^2 + S_{\Omega,y}^2) + \vec{S} \cdot \mathbf{A} \cdot \vec{I} \quad (1)$$

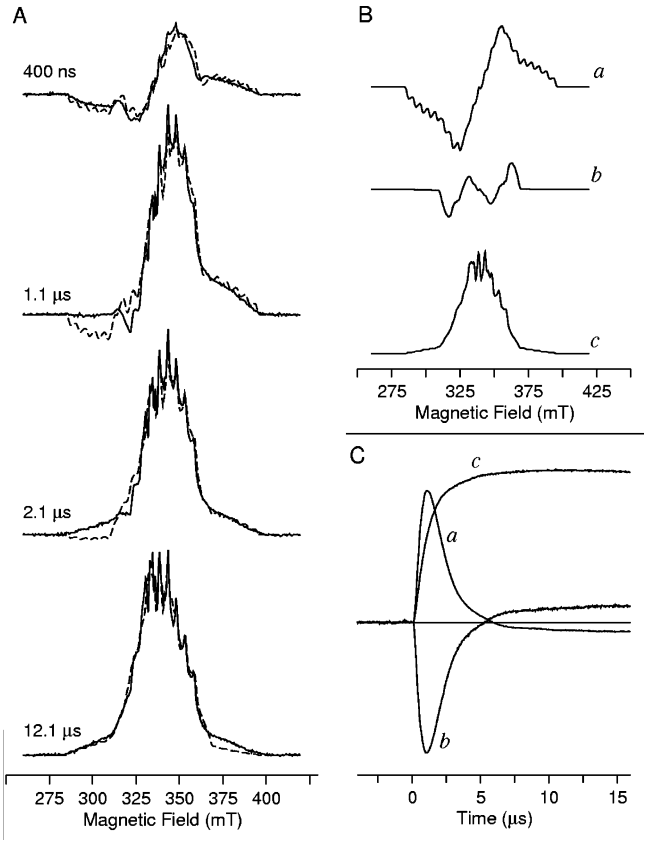

Figure 4. X-band (9 GHz) spin-polarized transient EPR spectra of vanadyl octaethylporphyin in the liquid crystal E7 with the director oriented perpendicular to the magnetic field. The spectra are taken under the same conditions and calculated as those shown in Figure 3.

where S and I refer to the electron and nuclear spins, respectively. The subscript Ω indicates that the operator is for a component of the spin in the molecular frame. To describe the spin polarization, i.e., the population distribution of the spin states of Hamiltonian (eq 1), we use the traceless reduced density matrix of the trip-quartet, $\Delta\rho$, written as a power series of the spin operators for the longitudinal magnetization with terms up to third order.[13,14] The even and odd terms of the series correspond to multiplet and net contributions to the polarization, respectively, and are denoted $\Delta\rho_M$ and $\Delta\rho_N$.

As discussed in the preceding paper,[26] the multiplet contribution is written as the sum of an axial and a nonaxial term given by:

$$\Delta\rho_M^{\text{axial}} \propto (1 - 3\cos^2\theta)(S_{Qz}{}^2 - (1/3)\vec{S}_Q{}^2)$$
$$\Delta\rho_M^{\text{nonaxial}} \propto \sin^2\theta\cos 2\phi(S_{Qz}{}^2 - (1/3)\vec{S}_Q{}^2) \qquad (2)$$

where θ and ϕ describe the orientation of the external field in the molecular frame. The operators are given in the laboratory frame and the subscript Q refers to the quartet spin. The net polarization is described[26] by two terms proportional to the operator S_z:

$$\Delta\rho_N(z) \propto \sin^2\theta\, S_{Qz}$$
$$\Delta\rho_N(xy) \propto \cos^2\theta\, S_{Qz} \qquad (3)$$

Here, we neglect the possible contribution from cubic terms, i.e., with the density matrix proportional and S_z.[3]

TABLE 1: Simulation Parameters

g-tensor	HFI tensor (mT)	zero-field splitting	order tensor
g_{zz} =1.988	A_{zz} = 5.40	D = 17.5 mT	S_{zz} = − 0.4
$g_{xx} = g_{yy}$ = 1.995	A_{xx}=A_{yy}=1.84	E = 1.5 mT	$S_{xx} - S_{yy}$ = 0

The relative importance of the four contributions to the density matrix $\Delta\rho$ depends on the mechanism by which the polarization is generated. Because this mechanism is not known in detail, we combine them using unknown weights κ_1, κ_2, κ_3, and κ_z and κ_{xy}, which are treated as time dependent adjustable parameters:

$$\Delta\rho(t) = \kappa_1(t)\Delta\rho_M^{\text{axial}} + \kappa_2(t)\Delta\rho_M^{\text{nonaxial}} + \kappa_3(t)\Delta\rho_N$$
$$\Delta\rho_N = \kappa_z\Delta\rho_N(z) + \kappa_{xy}\Delta\rho_N(xy) \qquad (4)$$

Because the angular dependence of the net contributions (eq 3) is weak, κ_z and κ_{xy} are strongly correlated and their time dependence is difficult to determine. To circumvent this problem, we assume their ratio, $\kappa = \kappa_z/\kappa_{xy}$, is time-independent. If this assumption is correct, the ratio is a property of the molecule. However, some variation between samples may be expected due to the influence of the solvent on the relative efficiency of the in-plane and out-of-plane components of the spin−orbit coupling.

The three time-independent contributions $\Delta\rho_M^{\text{axial}}$, $\Delta\rho_M^{\text{nonaxial}}$, and $\Delta\rho_N$ are given in panel B in Figures 2−4. The calculation of these contributions was carried out using the program described in the preceding paper.[26] The program models the continuous-wave magnetic resonance spectra for an arbitrary static spin-Hamiltonian in the linear approximation of the intensity of the microwave probing field and produces a stick spectrum which is then convoluted numerically with a Gaussian line shape. Here, Hamiltonian (eq 1) was used with the parameter values collected in Table 1. The orientation distribution used for the partially ordered samples is also described in detail in the preceding paper.[26] The ratio of the two net polarization contributions $\kappa = \kappa_z/\kappa_{xy}$ was determined by fitting the sum of the four spectra shown in panel A for each of Figures 2−4.

3.3. Time Dependence of the Net and Multiplet Polarization. The time dependence of the amplitudes of the three contributions is presented as three curves in panel C in Figures 2−4. For these curves, the value κ was held fixed and the time dependence of the coefficients $\kappa_1(t)$, $\kappa_2(t)$, and $\kappa_3(t)$ was determined by fitting the entire time/field dataset. The quality of the fit is demonstrated by the comparison between the experimental (solid curves) and calculated (dashed curves) spectra in several different time windows shown in panel A of Figures 2−4. The κ-coefficients obtained for these spectra are listed in Table 2. These values and the complete time dependence show that the multiplet polarization dominates immediately after the laser flash and then decays as the net polarization rises. The decay of the net polarization is approximately 3 orders of magnitude slower than its rise. Although the decay of the multiplet polarization and the rise of the net polarization are similar, they are not identical. Hence, they appear to be related, but the evolution of the polarization is more complex than just a direct transformation from one pattern to another.

This separation of the data into net and multiplet contributions that are correlated with different powers of the spin operators is important in understanding the origin of the polarization because the terms reflect the symmetry of different types of interactions. Processes internal to the molecule generally follow

TABLE 2: Weights of Different Polarization Patterns

window	κ_1	κ_2	κ_3	κ_z	κ_{xy}
X-band TREPR spectra in toluene at 15 K (Figure 1)					
0.3−0.5 μs	0.170	−0.144	0. 148	−0.878	0.122
1.0−1.2 μs	0.726	−0.347	0.484		
2.0−2.2 μs	0.732	−0.313	0.716		
12.0−12.2 μs	0.165	−0.077	0.994		
X-band TREPR spectra in E7 in parallel orientation at 15 K (Figure 2)					
0.3−0.5 μs	0.244	−0.581	0.123	−0.823	−0.177
2.0−2.2 μs	0.495	−0.418	0.765		
3.0−3.2 μs	0.252	−0.147	0.885		
12.0−12.2 μs	−0.069	−0.003	0.996		
X-band TREPR spectra in E7 in perpendicular orientation at 15 K (Figure 3)					
0.3−0.5 μs	0.348	−0.420	0.174	−0.799	−0.201
2.0−2.2 μs	0.553	−0.536	0.813		
3.0−3.2 μs	0.231	−0.219	0.889		
12.0−12.2 μs	−0.054	0.098	0.995		

TABLE 3: Inhomogeneous Gaussian Linewidths

	temperature			
solute	15 K	25 K	50 K	80 K
toluene	2.0 mT	2.0 mT	2.4 mT	2.4 mT
E7, isotropic	−	1.4 mT	1.4 mT	2.0 mT
E7, parallel	1.0 mT	−	1.0 mT	−
E7, perpendicular	1.4 mT	−	1.8 mT	−

even powers of the operators, whereas interactions with an external field follow the odd powers. This can be seen, for example, in Hamiltonian (eq 1) in which the Zeeman interaction scales as S_z whereas the zero-field splitting scales as S_Ω^2. Thus, because the multiplet polarization dominates initially, we surmise that the electronic transition to the quartet state follows the molecular symmetry as would be expected for spin−orbit coupling mediated intersystem crossing.

Another obvious fact from the data in Figures 3 and 4 (partially oriented samples) is that the multiplet polarization changes sign at about 5−6 μs after the laser flash. This can be seen in the fact that the coefficients of both multiplet contributions pass through zero at the same point. This observation is also supported by integrated spectra taken at 3 and 12 μs (Figures 3 and 4, panel A). In the time window at 3 μs, the right-hand side of the spectra is more intense because the multiplet and net contributions add in this region. The low-field side of the spectrum is weaker because the net and multiplet contributions cancel in this region. At 12 μs, this pattern is reversed and the low-field side is stronger because the sign of the multiplet contribution has changed.

3.4. Influence of the Dynamics on the Spectral Properties. The process that causes the change in the polarization patterns with time also affects some of the parameters used to simulate the spectra in Figures 2−4. The prinicipal values of the g-tensor, HFI tensor, ZFS tensor and order matrix are given in Table 1 and are independent of temperature and solvent. The line widths and the kinetic parameters on the other hand depend on the experimental conditions, and therefore, they are collected separately in Tables 3 and 4, respectively. Inspection of these two tables shows that the line width and the kinetic rates both increase with the temperature, suggesting that the processes causing the change in the polarization also broadens the spectra. In addition, the measurements taken in E7 show that the line width is orientation dependent and correlates with the zero-field splitting and hyperfine coupling. The *z*-components of the ZFS and HFI tensors are larger than the in-plane components, and they contribute primarily to the spectra when the director is perpendicular to the field. In Table 3, it can be seen that the line width is consistently larger for the perpendicular orientations as well. In the simulations, the axial contribution to the multiplet polarization shows a steplike pattern in the wings of the spectra that comes from the *z*-component of the hyperfine coupling (see Figure 4B, spectrum a). However, in the experimental spectrum, this pattern is not resolved. These observations suggest that back-and-forth transitions between the trip-quartet and trip-doublet states may broaden the spectrum of the trip-quartet by causing a shift in the resonance frequency. Such a shift is expected to be proportional to the magnitude of the zero-field and hyperfine splittings in the spectrum and the rate of the transitions. Hence, it would be largest when the molecular *z*-axis is parallel to the field.

3.5. Temperature Dependence of the Rise and Decay of the Net Polarization. The suggestion that time development of the polarization is due to transitions between the trip-quartet and trip-doublet is also supported by the small energy gap between trip-doublet and trip-quartet estimated from the temperature dependence of the decay rate of the net polarization.[26] The value of 47 cm^{-1} obtained from decay rates suggests that the thermal energy is sufficient to support transitions between the lowest excited trip-quartet and trip-doublet states, even at 15 K.

The rise and decay rates of the net contribution have been determined by summing the TREPR signal over the field range and fitting the resulting transient with a biexponential function. The values obtained from these fits are summarized in Table 4. Because the two rates differ by 3 orders of magnitude, the signal cannot be digitized with sufficient resolution to determine both rates from a single measurement; thus, different datasets with different digital resolution were used. The rise rates are based on the measurements of the first 16 μs with 25 ns/point, whereas the decay rates were obtained from a time window from 0.8 to 1.6 ms measured with 2.5 μs/point. For the later measurements, low-frequency background noise with a period in the range of several ms becomes difficult to subtract, and hence, the error in the decay rates is estimated to be 20−30%. The difficulties do not affect the signal at short times, and the error in the initial rise rate is estimated to be ∼5%. In some cases, the transients show evidence of more complex behavior than a simple biexponential process.

The rates from Table 4, averaged over a series of experiments at the same temperature, are presented as the corresponding lifetimes in Figure 5. The open circles are the initial rise (in microseconds) whereas the filled circles are the decay time (in milliseconds). As can be seen, both rates have similar temperature dependencies and only begin to slow dramatically below about 50 K. Thus, it is likely that they are both governed by the energy gap between the trip-doublet and trip-quartet states. However, the processes involved in determining the two rates are clearly very different.

In summary, the properties of the TREPR data clearly suggest that the spin-polarization reflects the internal dynamics of the excited states. Among the possible processes that could affect the polarization, the mostly likely candidate is the back-and-forth transitions between the trip-quartet and trip-doublet states.

4. Model

We now turn to the details of a model for the excited-state dynamics that should rationalize all of the above observations. The model is based on the idea that the back-and-forth transitions between the trip-doublet and trip-quartet states are

TABLE 4: Rise and Decay Rates of the Net Polarization[a]

	15 K		25 K		50 K		80 K	
rate solute	rise, $10^6\,s^{-1}$	decay $10^3\,s^{-1}$	rise, $10^6\,s^{-1}$	decay, $10^3\,s^{-1}$	rise, $10^6\,s^{-1}$	decay, $10^3\,s^{-1}$	rise, $10^6\,s^{-1}$	decay, $10^3\,s^{-1}$
toluene	0.74	–	1.13	–	1.44	–	1.56	5.4
E7, iso	–	1.2[b]	1.02	2.5	–	6.0	1.17	10.8[c]
E7, para	0.77	–	–	–	1.42	–	–	–
E7, perp	0.88	–	–	–	1.24	–	–	–

[a] The rates were obtained from a fit of the sum of the TREPR time traces at all field positions in the time/field dataset. [b] Determination of the decay rate was hampered by low-frequency noise in the experimental data. [c] The decay rate from optical measurements is $8.98 \times 10^3\ s^{-1}$. The TREPR time trace in center of the spectrum at 342 mT has a decay rate[26] of $7.70 \times 10^3\ s^{-1}$.

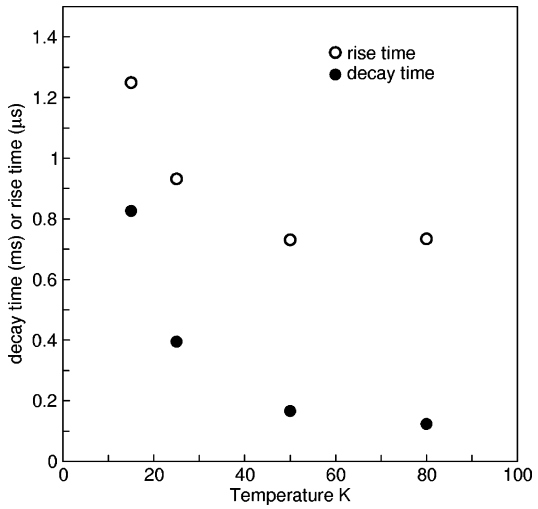

Figure 5. Temperature dependence of the spin polarization lifetime of OEPVO, the averaged summary over measurements at different temperatures and in different media. (○) Experimental values of the net polarization rise time at each temperature. (●) Experimental values of the signal decay time.

the origin of the evolution of the polarization. However, two main questions remain that are not straightforward to answer.

4.1. Requirements for the Model. The first challenge is to explain the origin of the net contribution generated during the detection of the signal. Under the conditions of the experiment, this problem is nontrivial because low temperature prevents any large-scale molecular motion, and therefore, variation of the exchange interactions can be ruled out. Because of this, the level crossing mechanism and other pathways referred as the triplet mechanism in the CIDEP literature are not efficient for this case. The polarization also cannot be generated by the mixing of states by precession of the spins because such mechanisms are effective only when the exchange interaction is similar to the differences of Zeeman interactions. This is clearly not the case in vanadyl porphyrin molecules. The only model that has been proposed to explain the polarization in such systems invokes spin-selective transitions between trip-doublet and trip-quartet states via spin−orbit coupling to explain both the net and the multiplet contributions of the polarization. It has been illustrated that a relatively weak Zeeman energy can lead to a noticeable contribution to the net polarization even in a strongly coupled molecular system.[13,14] We assume that this mechanism is dominant in the case of OEPVO.

The second problem is that even if the presence of net polarization can be explained by the influence of the Zeeman interaction on spin−orbit coupling ISC, we must still provide a rationalization for the complex time and temperature dependence of the TREPR signals. First, we must explain why the net polarization increases with time to become much larger than the initial multiplet polarization. Second, any proposed model must be consistent with the observation that the lifetime of the net polarization correlates with that of the trip-quartet state. In this context, an important additional observation is that the decay of the polarization was found to be independent of the microwave power within the available range. Moreover, transient nutations could not be induced despite the fact that under the same conditions they are observed for the triplet states of related molecules. We will show that all of these features are consistent with back-and-forth quartet-doublet transitions, which reduce the multiplet polarization and continually regenerate the net polarization.

4.2. Description of the States Involved. In the analysis of the EPR data presented above, the spectra were simulated using a spin Hamiltonian containing the Zeeman and spin−spin interactions. The populations were treated as unknown parameters. To calculate these populations, orbital terms must be included in the Hamiltonian because the polarization is generated by ISC, i.e., by transitions between electronic states. Here we consider only the trip-doublet and trip-quartet states of the two lowest excited electronic configurations as shown in Figure 1. In the Hamiltonian, we include a crystal field splitting term, H_Δ, to describe the orbital part of the energy gap between these states. The exchange interaction, J, between the triplet excitation and the unpaired vanadyl d-electron is also included and is taken to be independent of the orbital states. The zero-field and hyperfine interactions are assumed to have no significant influence on the transitions between the electronic states because their contribution to the energy is small. Hence, they are ignored in the calculation of the populations. The Zeeman interaction, on the other hand, cannot be ignored, despite the fact that it is also much smaller than the crystal field splitting and the exchange interaction, because it is responsible for the net polarization. The resulting Hamiltonian is then:

$$H = \omega(S_{T,z} + S_{VO,z}) - 2J\vec{S}_T\vec{S}_{VO} + H_\Delta \qquad (5)$$

where the subscripts T and VO indicate that the operators act on the triplet spin of the excited porphyrin ring and the doublet spin of the vanadyl ion, respectively, and z refers to the magnetic field direction in the laboratory frame.

Next, we need to consider the orbital part of the eigenstates of H and to define the operator H_Δ more precisely. The important feature of the two orbital states taken into account in the model is that they have E_u symmetry and transform as vectors along x and y. This also means they are mixed by the z-component of the spin−orbit coupling, which transforms as a rotation about the molecular z-axis. Following the strategy introduced by Canters and van der Waals,[31] we label these two states $|x\rangle$ and $|y\rangle$ and represent them with two orthogonal functions having the correct rotational symmetry:[32,33]

$$|x\rangle = \frac{1}{\sqrt{2}}(|L,-1\rangle - |L,1\rangle)$$

$$|y\rangle = \frac{i}{\sqrt{2}}(|L,-1\rangle + |L,1\rangle) \quad (6)$$

We use the letter L to indicate that the states are associated with different projections of the orbital angular momentum of the excited π-orbital of porphyrin ring. The corresponding operator L_z acts as a rotation and transforms $|x\rangle$ into $|y\rangle$ and vice versa. To describe the crystal field interaction H_Δ, we require an operator that splits these states by an energy gap Δ:

$$\langle x|H_\Delta|x\rangle = 0$$

$$\langle y|H_\Delta|y\rangle = \Delta \quad (7)$$

Because the operator L_x^2 has the properties $\langle x|L_x^2|x\rangle$ and $\langle y|L_x^2|y\rangle$, it is convenient to define the operator $H_\Delta = \Delta L_x^2$.

The exchange interaction between the triplet and doublet splits each of the two orbital states into a trip-doublet and trip-quartet, giving the four low-lying excited electronic states $|D,x\rangle$, $|Q,x\rangle$, $|D,y\rangle$ and $|Q,y\rangle$. Finally, the doublet and quartet states further split by the Zeeman interaction into spin states with different projections as shown in Figure 1.

At this point, it is important to discuss the consequences of these approximations. By only including the two low-lying orbital components, the main features of the system including the spectral, temporal, and thermal properties can be described analytically. However, with this restriction, the model does not reproduce all of the observed properties of the TREPR spectra. In particular, it cannot generate the population distribution that leads to the nonaxial component of the multiplet polarization $\Delta\rho_M^{nonaxial}$ and the in-plane component of the net polarization $\Delta\rho_N(xy)$. However, this restriction can be overcome by a straightforward expansion of the description to include other orbital configurations, if the parameters of interactions are known. Here, we use only the simplified model, and hence, the calculation only gives a qualitative description of the features of the observed spin polarization.

4.3. Introduction of SO Coupling and Rate Constants. Next, we introduce spin−orbit coupling as a perturbation that mixes the eigenstates of and thus mediates ISC between the trip-doublet and trip-quartet manifolds. For simplicity, we assume that this mixing represents only a small perturbation of the spin eigenstates and that the unperturbed energies may be used. This approach should be valid for weak spin−orbit coupling and greatly simplifies the resulting expressions for the rates and the populations of the states. A more rigorous treatment is given elsewhere.[13,14] In addition, we assume that $|x\rangle$and $|y\rangle$ are well separated energetically from all other orbitals, and therefore, only mixing between the trip-doublet and trip-quartet states shown in Figure 1 is significant. Hence, we retain only the z-component of spin−orbit coupling, which mixes $|x\rangle$ and $|y\rangle$. Although the symmetry of the spin polarization patterns suggests that the x- and y-components of spin−orbit coupling also play a role, they can be described using the results obtained for the z-component by simply redefining the axes. Here, the perturbing spin−orbit coupling is expressed as

$$H\lambda = \lambda S_\Omega, TzL_z \quad (8)$$

Here λ is the strength of the interaction between the spin angular momentum of the triplet excitation of the porphyrin ring and the orbital angular momentum of $|x\rangle$ and $|y\rangle$; the symbol Ω is used to indicate the molecular reference system of the spin states.

Because the energy gap between the initial and final states is small, the usual description of electronic relaxation via transitions into a continuum of vibronic states does not apply to decay from the lowest trip-doublet state to the lowest trip-quartet. Instead, this process involves mixing of $|D,x\rangle$ and$|Q,y\rangle$ by spin−orbit coupling followed by fast internal conversion of $|Q,y\rangle$ to $|Q,x\rangle$. Therefore we expect that the rate of doublet-quartet ISC can be expressed as the product of the rate of internal conversion and the degree of mixing between $|D,x\rangle$ and $|Q,y\rangle$:

$$k_{ij} = k_0|\langle D_i,x|H_\lambda|Q_j,y\rangle|^2/(E(D_i,x) - E(Q_j,y))^2 \quad (9)$$

Here $|D_i,x\rangle$ is the spin sublevel of the trip-doublet in orbital state $|x\rangle$ from which the transition takes place and $|Q_j,y\rangle$ is the spin sublevel of the trip-quartet state in orbital state $|y\rangle$, k_0 is the rate of spin independent internal conversion from $|y\rangle$ to the $|x\rangle$; $E(D_i,x)$ and $E(Q_j,y)$ are the corresponding energies of levels i and j. An analogous expression can be written for transitions in the opposite direction, i.e., from the lowest trip-quartet to the lowest trip-doublet, and is obtained by substituting the appropriate wave functions and energies in (eq 9).

4.4. Rate Equations. The rate constants obtained from (eq 9) can then be used in the set of kinetic rate equations

$$\partial\vec{n}/\partial t = \mathbf{K}\cdot\vec{n} \quad (10)$$

for the spin populations of the lowest trip-doublet and trip-quartet states $|D,x\rangle$ and $|Q,x\rangle$:

$$\vec{n} = (n_{D,-1/2}\ \ n_{D,+1/2}\ \ n_{Q,-3/2}\ \ n_{Q,-1/2}\ \ n_{Q,+1/2}\ \ n_{Q,+3/2})^{tr} \quad (11)$$

where the superscript tr indicates the transpose, i.e., $\vec{n}$ is a column vector. The diagonal elements of the rate constant matrix $\mathbf{K}$ describe transitions *from* each of the sublevels and therefore are negative, whereas the off-diagonal elements describe transitions *to* them and are positive. If the decay to the ground state is also taken into account, the matrix of rate constants, $\mathbf{K}$, can be written as the sum of three contributions:

$$\mathbf{K} = \mathbf{K}_G + \mathbf{K}_{DQ} + \mathbf{K}_\omega \quad (12)$$

$\mathbf{K}_G$ is the rate of relaxation to the ground state whereas $\mathbf{K}_{DQ}$ and $\mathbf{K}_\omega$ are different contributions to the rate constants obtained from eq 9. The contribution described by $\mathbf{K}_{DQ}$ arises from the interactions that follow the molecular symmetry, whereas $\mathbf{K}_\omega$ contains the terms that depend on the Zeeman energy, ω. For experiments at X-band, ω is expected to be small compared to the splitting between electronic states, i.e., $\omega \ll \Delta - 3J$, $\Delta + 3J$. Under these conditions, we obtain the following expressions for $\mathbf{K}_G$, $\mathbf{K}_{DQ}$, and $\mathbf{K}_\omega$:

$$\mathbf{K}_G = \begin{pmatrix} -k_{DG} & 0 & 0 & 0 & 0 & 0 \\ 0 & -k_{DG} & 0 & 0 & 0 & 0 \\ 0 & 0 & -k_{QG} & 0 & 0 & 0 \\ 0 & 0 & 0 & -k_{QG} & 0 & 0 \\ 0 & 0 & 0 & 0 & -k_{QG} & 0 \\ 0 & 0 & 0 & 0 & 0 & -k_{QG} \end{pmatrix} \tag{13}$$

$$\mathbf{K}_{DQ} = \begin{pmatrix} -2k_{DQ} & 0 & (3/2)k_{QD}\sin^2\theta & 2k_{QD}\cos^2\theta & (1/2)k_{QD}\sin^2\theta & 0 \\ 0 & -2k_{DQ} & 0 & (1/2)k_{QD}\sin^2\theta & 2k_{QD}\cos^2\theta & (3/2)k_{QD}\sin^2\theta \\ (3/2)k_{DQ}\sin^2\theta & 0 & -(3/2)k_{QD}\sin^2\theta & 0 & 0 & 0 \\ 2k_{DQ}\cos^2\theta & (1/2)k_{DQ}\sin^2\theta & 0 & -(1/2)k_{QD}(1+3\cos^2\theta) & 0 & 0 \\ (1/2)k_{DQ}\sin^2\theta & 2k_{DQ}\cos^2\theta & 0 & 0 & -(1/2)k_{QD}(1+3\cos^2\theta) & 0 \\ 0 & (3/2)k_{DQ}\sin^2\theta & 0 & 0 & 0 & -(3/2)k_{QD}\sin^2\theta \end{pmatrix} \tag{14}$$

$$\mathbf{K}_\omega = \sin^2\theta \begin{pmatrix} -\eta_{DQ} & 0 & -(3/2)\eta_{QD} & 0 & (1/2)\eta_{QD} & 0 \\ 0 & \eta_{DQ} & 0 & -(1/2)\eta_{QD} & 0 & (3/2)\eta_{QD} \\ (3/2)\eta_{DQ} & 0 & (3/2)\eta_{QD} & 0 & 0 & 0 \\ 0 & (1/2)\eta_{DQ} & 0 & (1/2)\eta_{QD} & 0 & 0 \\ -(1/2)\eta_{DQ} & 0 & 0 & 0 & -(1/2)\eta_{QD} & 0 \\ 0 & -(3/2)\eta_{DQ} & 0 & 0 & 0 & -(3/2)\eta_{QD} \end{pmatrix} \tag{15}$$

where the angle θ describes the orientation of the molecular z-axis relative to the space-fixed Z-axis. The rates constants k_{DQ}, k_{QD}, η_{DQ}, and η_{QD} describing the back-and-forth transitions between the trip-doublet and trip-quartet are given by:

$$k_{DQ} = \frac{\lambda^2}{9(\Delta - 3J)^2}k_0\, k_{QD} = \frac{\lambda^2}{9(\Delta + 3J)^2}k_0 e^{-3J/kT}$$

$$\eta_{DQ} = \frac{2\omega}{\Delta - 3J}k_{DQ}\, \eta_{QD} = \frac{2\omega}{\Delta + 3J}k_{QD} \tag{16}$$

In eq 16, we add a Boltzmann factor for transitions from the trip-quartet to the trip-doublet on the basis of the energy difference between these states assuming $\omega \ll 3J$. This factor reflects the difference in the rates of the back-and-forth transitions between the lowest trip-doublet and trip-quartet states if they are in thermal equilibrium.

In matrixes 14 and 15, inspection of the elements corresponding to the kinetic equations for the trip-quartet sublevels (bottom four rows of the matrixes) shows that $\mathbf{K}_{DQ}$ and $\mathbf{K}_\omega$ describe the kinetics of the multiplet and net polarization, respectively. This can be seen, for example, in the fact the elements of $\mathbf{K}_{DQ}$ for the $\pm 1/2$ sublevels of the trip-quartet (rows 4 and 5) have the same form and are different from those for the $\pm 3/2$ levels (rows 3 and 6). The trace of $\mathbf{K}_\omega$ is zero; hence, these terms create only *differences* in the rates for the various transitions whereas the sum of the rates remains the same. It is these differences in rate that generate the net polarization. For example, the contribution from $\mathbf{K}_\omega$ increases the rate of transitions *from* the $+1/2$ and $+3/2$ sublevels of the quartet whereas the rate of transitions *to* these levels are decreased. The opposite effect is found for the $-1/2$ and $-3/2$ sublevels. This is also reflected in the fact that $\mathbf{K}_\omega$ is antisymmetric about the diagonal. For instance, the contribution from $\mathbf{K}_\omega$ increases the rate constant for the transition from $D_{-1/2} \rightarrow Q_{+1/2}$ by an amount $\mathbf{K}_\omega,1,5 = \eta_{DQ}/2$ whereas the rate of reverse process $Q_{+1/2} \rightarrow D_{-1/2}$ is decreased by $\mathbf{K}_\omega,5,1 = -\eta_{QD}/2$. These differences in the rates effectively describe a change in the spin orientation during ISC.

The solution $\vec{n}$ (eq 12) of kinetic equations (eq 11) represent the populations of the trip-doublet D_x and trip-quartet Q_x states. From this vector we can derive the corresponding density matrixes. For the quartet state this is:

$$\rho_Q = \begin{pmatrix} n_{Q,-3/2} & 0 & 0 & 0 \\ 0 & n_{Q,-1/2} & 0 & 0 \\ 0 & 0 & n_{Q,1/2} & 0 \\ 0 & 0 & 0 & n_{Q,3/2} \end{pmatrix} \tag{17}$$

To obtain the polarization of the quartet state, we rewrite ρ_Q in operator form and take the traceless part of the density matrix:

$$\Delta\rho_Q = p_1 S_{Qz} + p_2(S_{Qz} - (1/3)\vec{S}_Q{}^2) + p_3 S_{Qz}{}^3 \tag{18}$$

The coefficients p_1 and p_3 are the net polarization and p_2 is the multiplet polarization.

4.5. Numerical Calculations of the Time Dependence of the Polarizations. Figure 6 shows the net and multiplet contributions to the polarization obtained from a numerical solution of the kinetic equations (eq 11). The polarization is expressed as a percentage of the total population calculated for the sum over an isotropic distribution of molecular orientations. Because negative polarization (i.e., greater population in the sublevels of lower energy) results in an absorptive (positive) EPR signal, the polarization is plotted with negative values on the ordinate axis in Figure 6. For the calculation, the exchange integral J is estimated to be 16 cm^{-1} (1/3 of 47 cm^{-1} [26]) and $\omega = 0.3$ cm^{-1}. The value of Δ is unknown, but we expect it to be in the range of several tens of wavenumbers, and a value of $\Delta = 60$ cm^{-1} has been chosen arbitrarily. The values of the other parameters used in the calculation are given in the caption to Figure 6. As can be seen, the model reproduces the main features of the observed polarization, with net polarization (solid, p_1 and dotted curves, p_1+p_3) being generated, whereas the multiplet polarization (dashed curve, p_2) decays and changes sign. In addition, the two net polarization curves show that the contribution from the third-order term, p_3, is relatively weak and that truncation after the linear term is a reasonable approximation.

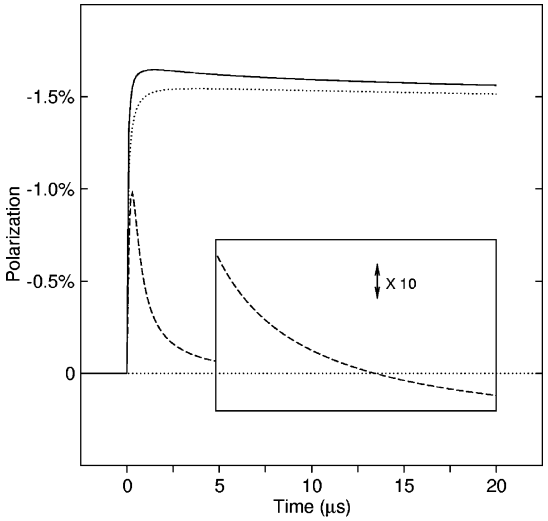

Figure 6. Time-dependence of the contributions to the polarization of the quartet state. The solid, dotted, and dashed curves correspond to the coefficients p_1, p_1+p_3, and p_2 of the operators S_{Qz}, $S_{Qz} + S_{Qz}^3$, and $S_{Qz}^2 - (1/3)\vec{S}_Q^2$, respectively (see eq 18). The first two of these describe the net contribution, whereas $S_{Qz}^2 - (1/3)\vec{S}_Q^2$ is the multiplet polarization of the quartet state. The curves in the inserted frame are enlarged by a factor of 10 to demonstrate the change of sign of mutiplet polarization. The polarization contributions are derived from numerical solutions of the kinetic equations (eq 11) with initial populations $\vec{n}_0 = (1,1,0,0,0,0)/2$ corresponding to unpolarized population of the trip-doublet state. The solutions of (eq 10) were averaged over isotropic distribution of molecular orientations. The exchange interaction $J = 16$ cm^{-1}, $k_{DG} = 0.05 \times 10^6$ s^{-1}, and $k_{QG} = 0.94 \times 10^3$ s^{-1} were estimated from the temperature dependence of the TREPR spectra discussed in the preceding paper.[26] The temperature $T = 15$ K and the Zeeman energy $\omega = 0.3$ cm^{-1} (X-band) correspond to the conditions used for the experiments summarized in Figures 2−4. The value of the spin−orbit coupling, λ, and the rate of IC, k_0, act jointly (eq 17) and determine the rate of the back-and-forth transitions between the trip-quartet and trip-doublet. We choose them as 3 cm^{-1} and 10^{13} s^{-1}, respectively. The energy gap, Δ, between the orbitals $|x\rangle$ and $|y\rangle$ (eq 6) is arbitrarily set to 60 cm^{-1}.

Unlike the experimental data, the calculations give only one multiplet contribution because we have considered only the contribution of the *z*-component of the spin−orbit coupling (see eq 18).

Experimentally, we find that the decay to the ground state is several orders of magnitude slower than the rise of the net polarization. Hence, the observed polarization at late times should correspond approximately to the stationary conditions when $k_{DG} = k_{QG} = 0$. Under these conditions, we obtain for the stationary populations, $\vec{n}_0$:

$$\vec{n}_0 = \frac{1}{4}\left(\frac{k_{QD}}{k_{DQ}}(1+2\eta), \frac{k_{QD}}{k_{DQ}}(1+\eta), 1+3\eta, 1+2\eta, 1+\eta, 1\right)^{tr}$$

$$\eta = (1/2)\sin^2\theta(\eta_{DQ}/k_{DQ} + \eta_{QD}/k_{QD}) = \frac{2\omega\Delta}{\Delta^2 - 9J^2}\sin^2\theta \quad (20)$$

Thus, η represents the maximal value of the quartet polarization, and it can be calculated from the parameters used for Figure 6. The angular dependence integrated over the unit sphere gives $\langle\sin^2\theta\rangle = 2/3$. With $\Delta = 60$ cm^{-1}, we obtain $\langle\eta\rangle \approx 2\%$. This value can be compared to the Boltzmann factor at 15 K, which gives a polarization of ~3%. The observed polarization of the trip-quartet is much larger than that of the ground state at thermal equilibrium although a quantitative measure of the relative magnitudes of their EPR spectra is difficult to obtain. Thus, with the parameters chosen for Figure 6, the model appears to give a polarization of the quartet-state that is weaker than observed.

It is possible that this is because we have neglected in-plane components of the spin−orbit coupling and higher order perturbation terms.[13,14] However, the inverse dependence of the net polarization on the energy gap between lowest excited trip-doublet and the next excited trip-quartet state plays a more important role in determining the strength of the net polarization. Within the framework of the model, this energy gap, $\Delta - 3J$, must be small if strong net polarization is to be produced. Therefore, Δ should not differ greatly from the value of $3J = 47$ cm^{-1} estimated from the temperature dependence of the luminescence and spin-polarization lifetimes. The strong dependence of the net polarization on the relative magnitudes of Δ and $3J$ also provides a logical explanation of why the trip-quartet is not observed in copper porphyrins, because even a modest increase in $|\Delta - 3J|$ leads to a significant drop in the strength of the polarization. For instance, if this value is increased from 13 to 53 cm^{-1}, the polarization (eq 19) drops from 2 to 0.5%. The values of J that have been reported for copper porphyrins[25] are significantly larger than for OEPVO which would be consistent with weaker net polarization. However, because the relative magnitude of Δ in OEPVO and the copper porphyrins is not known, the effect of the difference in J on the polarization cannot be predicted with confidence.

4. Concluding Remarks

The kinetic model based on the spin−orbit mixing trip-doublet and trip-quarter states unifies the large set of spectral and temporal data on OEPVO in different solutes at several temperatures. As we have shown, all of the observed properties of the polarization and experimental parameters are consistent with this model. The main feature of the model is that the symmetry of the spin−orbit coupling leads initially to over population of the $\pm1/2$ sublevels of the trip-quartet, which gives the initial multiplet pattern and weak net polarization. The back-and-forth transitions to the trip-doublet, which are also governed by spin−orbit coupling, then deplete the $\pm1/2$ sublevels, leading to a decrease in the multiplet polarization and accumulation of net polarization. As shown in Figures 2−4 the multiplet polarization changes sign at late times under some conditions (compare Figures 2 and 3). Whether or not the multiplet polarization changes sign depends on how strongly the population of the $\pm1/2$ sublevels is depleted relative to the $\pm3/2$ sublevels. Within the model, both the decay to the ground state and the back-and-forth transitions between the excited states result in such a depletion. However, our calculations indicate that the change in sign of the multiplet polarization is predicted only if the decay rates to the ground state are nonzero.

Another feature of the model is that it suggests that a local spin temperature is maintained in the trip-quartet as a result of the back-and-forth transitions to the trip-doublet. In this context, an important parameter is the spin−lattice relaxation time, T_1. The excited-state dynamics make it difficult to obtain a reliable value for T_1 for the trip-quartet. However, the frequency and temperature dependence of spin−lattice relaxation for the ground state of a vanadyl porphyrin has been reported in the literature.[34] At 15 K, the observed T_1 for the ground state is about an order of magnitude longer than the lifetime of the net polarization shown in Figure 5 (●). Thus, it is probable that in trip-quartet, decay to the ground state is faster than spin lattice relaxation at 15 K. At 80 K, the ground-state T_1 is comparable to the trip-

quartet lifetime. In general, T_1 is expected to be shorter in the trip-quartet than in the ground state because the zero-field splitting provides an additional relaxation mechanism. Thus, it is likely that for temperatures above ~80 K, T_1 in the trip-quartet is shorter than the spin-polarization lifetime. From this, it appears that the decay of the spin polarization is independent of T_1, as would be expected if the polarization is maintained by the back-and-forth transitions between the excited states. Consistent with this, transient nutations could not be induced at high microwave power. Together, these observations support the idea that internal processes maintain the spin temperature in the excited states.

Acknowledgment. This work was supported by the Natural Sciences and Engineering Research Council (NSERC) and by two Grants-In-Aid for Scientific Research from JSPS, No. 11694061: (International Joint Research, B) and No. 13640554.

References and Notes

(1) Levanon, H.; Mobius, K. *Annu. Rev. Biophys. Biomol. Struct.* **1997**, *26*, 495.
(2) Stehlik, D.; Mobius, K. *Annu. Rev. Phys. Chem.* **1997**, *48*, 745.
(3) Conti, F.; Corvaja, C.; Toffoletti, A.; Mizuochi, N.; Ohba, Y.; Yamauchi, S.; Maggini, M. *J. Phys. Chem. A* **2000**, *104*, 4962.
(4) Franco, L.; Mazzoni, M.; Corvaja, C.; Gubskaya, V. P.; Berezhnaya, L. S.; Nuretdinov, I. A. *Chem. Commun.* **2005**, 2128.
(5) Mizuochi, N.; Ohba, Y.; Yamauchi, S. *J. Chem. Phys.* **1999**, *111*, 3479.
(6) Teki, Y.; Miyamoto, S.; Iimura, K.; Nakatsuji, M.; Miura, Y. *J. Am. Chem. Soc.* **2000**, *122*, 984.
(7) Teki, Y. *Polyhedron* **2001**, *20*, 1163.
(8) Yamauchi, S. *Bull. Chem. Soc. Jpn.* **2004**, *77*, 1255.
(9) van der Est, A.; Asano-Someda, M.; Ragogna, P.; Kaizu, Y. *J. Phys. Chem. A* **2002**, *106*, 8531.
(10) Rozenshtein, V.; Berg, A.; Levanon, H.; Krueger, U.; Stehlik, D.; Kandrashkin, Y.; van der Est, A. *Isr. J. Chem.* **2003**, *43*, 373.
(11) Saiful, I. S. M.; Fujisawa, J.; Kobayashi, N.; Ohba, Y.; Yamauchi, S. *Bull. Chem. Soc. Jpn.* **1999**, *72*, 661.
(12) Kawai, A.; Watanabe, Y.; Shibuya, K. *Mol. Phys.* **2002**, *100*, 1225.
(13) Kandrashkin, Y. E.; van der Est, A. *Chem. Phys. Lett.* **2003**, *379*, 574.
(14) Kandrashkin, Y. E.; van der Est, A. *J. Chem. Phys.* **2004**, *120*, 4790.
(15) Ishii, K.; Takeuchi, S.; Kobayashi, N. *J. Phys. Chem. A* **2001**, *105*, 6794.
(16) Ishii, K.; Ishizaki, T.; Kobayashi, N. *J. Chem. Soc., Dalton Trans.* **2001**, 3227.
(17) Ishii, K.; Fujisawa, J.; Ohba, Y.; Yamauchi, S. *J. Am. Chem. Soc.* **1996**, *118*, 13079.
(18) Ishii, K.; Bottle, S. E.; Shimizu, S.; Smith, C. D.; Kobayashi, N. *Chem. Phys. Lett.* **2003**, *370*, 94.
(19) Hugerat, M.; A. van der Est; E. Ojadi; L. Biczok; H. Linschitz; Levanon, H.; Stehlik, D. *J. Phys. Chem.* **1996**, *100*, 495.
(20) Fujisawa, J.; Ohba, Y.; Yamauchi, S. *Chem. Phys. Lett.* **1998**, *282*, 181.
(21) Asano-Someda, M.; Toyama, N.; Kaizu, Y. *Appl. Magn. Reson.* **2003**, *23*, 393.
(22) Asano-Someda, M.; van der Est, A.; Krüger, U.; Stehlik, D.; Kaizu, Y.; Levanon, H. *J. Phys. Chem. A* **1999**, *103*, 6704.
(23) Stavitski, E.; Berg, A.; Ganguly, T.; Mahammed, A.; Gross, Z.; Levanon, H. *J. Am. Chem. Soc.* **2004**, *126*, 6886.
(24) Kandrashkin, Y. E.; Asano, M. S.; van der Est, A. *Phys. Chem. Chem. Phys.* **2006**, *8*, 2129−2132.
(25) Gouterman M.; Mathies, R. A.; Smith, B. E.; Caughey, W. S. *J. Chem. Phys.* **1970**, *52*, 3795.
(26) Kandrashkin, Y. E.; Asano, M. S.; van der Est, A. *J. Phys. Chem. A* **2006**, *110*, 9607.
(27) Salikhov, K. M.; Molin, Y. N.; Sagdeev, R. Z.; Buchachenko, A. L. *Spin Polarization and Magnetic Effects in Radical Reactions*; Elsevier: Amsterdam, 1984.
(28) Asano, M.; Kaizu, Y.; Kobayashi, N. *J. Chem. Phys.* **1988**, *89*, 6567.
(29) Ishii, K.; Fujisawa, J.; Adachi, A.; Yamauchi, S.; Kobayashi, N. *J. Am. Chem. Soc.* **1998**, *120*, 3152.
(30) Sartori, E.; Garlaschelli, L.; Toffoletti, A.; Corvaja, C.; Maggini, M.; Scorrano, G. *Chem. Commun.* **2001**, *4*, 311.
(31) Canters, G. W.; van der Waals, J. H. High-Resolution Zeeman Spectroscopy of Metalloporphyins. In *The Porphyrins*; Dolphin, D., Ed.; Academic Press: New York, 1978; Vol. III, p 531.
(32) van der Poel, W.; Nuijs, A. M.; Noort, M.; van der Waals, J. H. *J. Phys. Chem.* **1982**, *86*, 5191.
(33) van der Waals, J. H.; van Dorp, W. G.; Schaafsma, T. J. Electron Spin Resonance of Porphyrin Excited States. In *The Porphyrins*; Dolphin, D., Ed.; Academic Press: New York, 1979; Vol. IV, p 257.
(34) Eaton, S. S.; Harbridge, J.; Rinard, G. A.; Eaton, G. R.; Weber, R. T. *Appl. Magn. Reson.* **2001**, *20*, 151.